1-1-1964

Calibration of Irrigation Headgates by Model Analysis

Gaylord V. Skogerboe

Vaughn E. Hansen

CALIBRATION OF IRRIGATION HEADGATES

BY MODEL ANALYSIS

Prepared by

Gaylord V. Skogerboe
and
Vaughn E. Hansen

March 1964

Performed for the

D. M. A. D. Company
Delta, Utah

by the

Engineering Experiment Station
College of Engineering
Utah State University
Logan, Utah

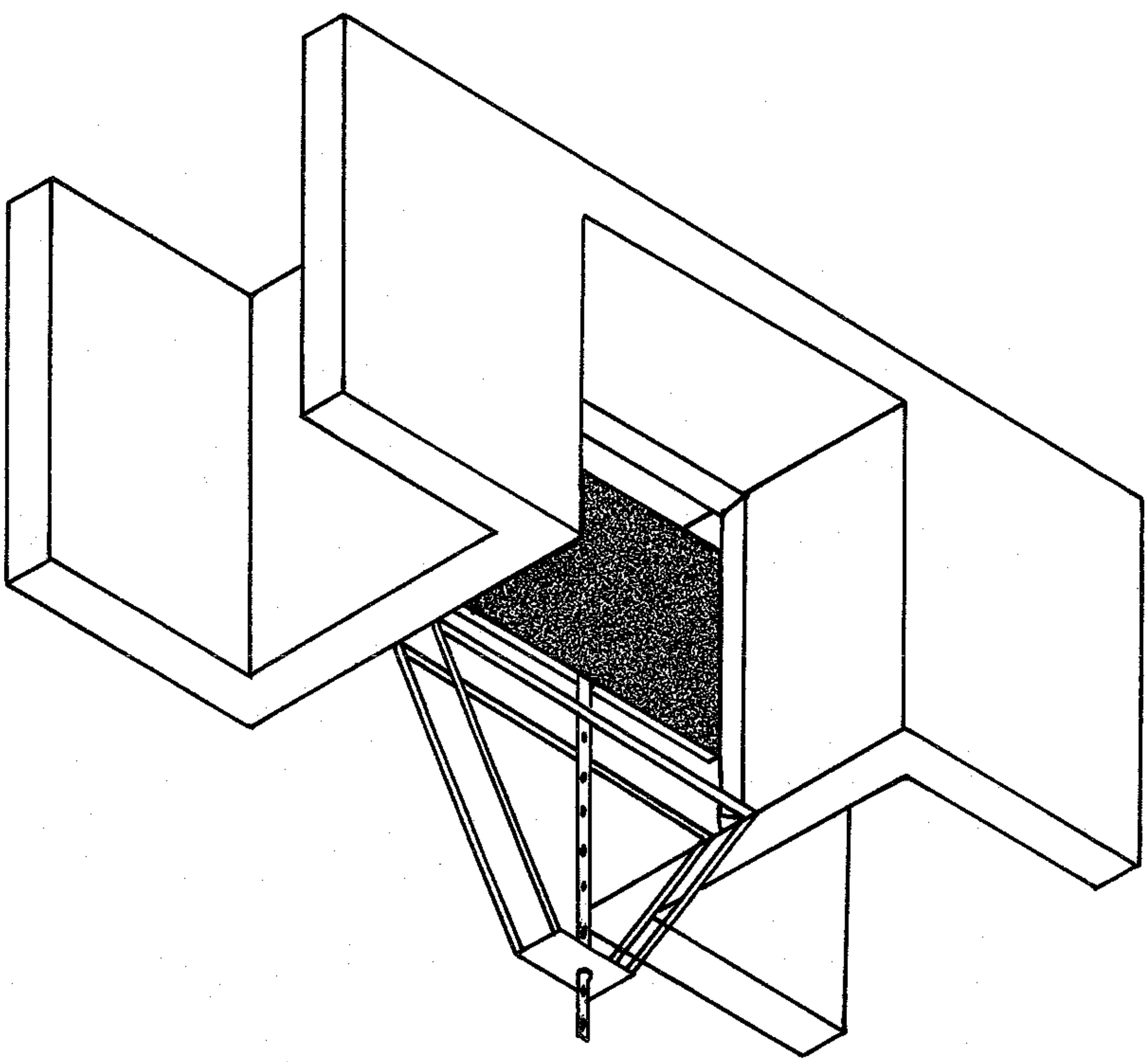

PROJECT PERSONNEL

Vaughn E. Hansen, Director, Engineering Experiment Station. Acted as project leader and gave guidance and direction to the research project.

C. Earl Israelsen, Research Engineer. Supervised the construction of the model and the initial tests.

Gaylord V. Skogerboe, Assistant Research Engineer. Replaced Mr. Israelsen after he left to continue his education at the University of Arizona

Mohammed Abaza, Graduate Assistant. Assisted in the construction of the model and in the testing program.

Shi-An Tsong, Graduate Assistant. Assisted in the laboratory throughout the testing program.

Teh-Chung Pai, Graduate Assistant. Assisted in the laboratory during the testing program.

Joe D. England, Student Assistant. Prepared the drawings and graphs in the report and assisted in the computational work.

Lawrence Robinson, Student Assistant. Assisted in the computational work.

ACKNOWLEDGEMENTS

We wish to express our sincere appreciation to the D. M. A. D. Company, and particularly to N. S. Bassett and Roger Walker, for their cooperation throughout this study. We were impressed by the depth of knowledge displayed by these gentlemen regarding the flow characteristics of the gate structures reported herein.

Counsel and suggestions were offered by many of the staff of the Engineering Experiment Station throughout the research program. The suggestions offered by Dr. Cheng-lung Chen, Professor Joel Fletcher, and Dr. Gordon H. Flammer were particularly helpful.

Gaylord V. Skogerboe

Vaughn E. Hansen

TABLE OF CONTENTS

LIST OF FIGURES

LIST OF TABLES

NOMENCLATURE

Symbol	Definition
A	Area of gate opening, sq. ft.
A_p	Area of gate opening in prototype, sq. ft.
A_m	Area of gate opening in model, sq. ft.
A_r	Ratio of A_p/A_m, dimensionless
b	Height of gate opening, ft.
b_p	Height of gate opening in prototype, ft.
b_m	Height of gate opening in model, ft.
b_r	Ratio of b_p/b_m, dimensionless
C_d	Coefficient of discharge, dimensionless
C_F	A coefficient defined by $C_F = 1.41C_d$, dimensionless
C_Q	A coefficient defined by $C_Q = AC_d(2g)^{1/2}$, $ft.^{5/2}/sec.$
F	Froude number, dimensionless
F_b	Froude number defined by $F_b = \frac{Q}{wb(gb)^{1/2}}$, dimensionless
g	Acceleration due to gravity, ft/sec^2
H_d	Depth of flow downstream from the gate after full recovery of kinetic energy has occurred and using the gate sill as a datum, ft.
$(H_d)_p$	Depth of flow in the prototype measured downstream from the gate after full recovery and using the gate sill as a datum, ft.
$(H_d)_m$	Depth of flow in the model measured downstream from the gate after full recovery and using the gate sill as a datum, ft.
H_u	Depth of flow upstream from the gate and using the gate sill as a datum, ft.
$(H_u)_p$	Depth of flow in the prototype upstream from the gate and using the gate sill as a datum, ft.

$(H_u)_p$	Depth of flow in the prototype upstream from the gate and using the gate sill as a datum, ft.
$(H_u)_m$	Depth of flow in the model upstream from the gate and using the gate sill as a datum, ft.
ΔH	Difference in water surface levels upstream and downstream from the gate, $H_u - H_d$, ft.
$(\Delta H)_p$	Difference in water surface levels in the prototype upstream and downstream from the gate, $(H_u)_p - (H_d)_p$, ft.
$(\Delta H)_m$	Difference in water surface levels in the model upstream and downstream from the gate, $(H_u)_m - (H_d)_m$, ft.
L	A length, ft.
L_p	A length in the prototype, ft.
L_m	A length in the model, ft.
L_r	Ratio of a length in the prototype to the corresponding length in the model, L_p/L_m, dimensionless
Q	Discharge, cfs
Q_p	Discharge in the prototype, cfs
Q_m	Discharge in the model, cfs
Q_r	Ratio of discharge in the prototype to the corresponding discharge in the model, Q_p/Q_m, dimensionless
s	Slope, dimensionless
V	Average velocity, ft/sec
V_p	Average velocity in the prototype, ft/sec
V_m	Average velocity in the model, ft/sec
V_r	Ratio of average velocity in the prototype to the corresponding average velocity in the model, V_p/V_m, dimensionless
w	Width of gate opening, ft.
w_p	Width of prototype gate opening, ft.
w_m	Width of model gate opening, ft.

CALIBRATION OF IRRIGATION HEADGATES BY MODEL ANALYSIS

INTRODUCTION

The purpose of this research project was to calibrate the slide gates used by the D. M. A. D. Company (Delta, Melville, Abraham and Deseret Irrigation Companies). These gates, which number more than 600, are located throughout the distribution system. Each gate is placed in a concrete box 4 feet wide, 3-1/2 feet deep and 4 feet long. The structure is used as a means of diverting the water and is also used as a measuring device.

A similar structure, but with a different type of slide gate, was calibrated in 1914. At that time rating tables were prepared which listed the flow rate when the height of gate opening and the difference in water levels upstream and downstream from the gate were know.

A number of measurements of flow through the present structures have been made in the field. These measurements have been utilized to relate the height of gate opening, b, and the difference in water levels upstream and downstream from the gate, ΔH, to the discharge rate, Q. Discharge rates were obtained by current meter measurements and were checked by making a systems analysis of the flow throughout the distribution system.

The water users have recognized for some time many of the problems inherent in calibrating these structures in the field. One of the primary difficulties is caused by the scour holes which have been formed immediately downstream from most of the structures. The depth of flow downstream from the gate has had to be observed at the scour hole because the concrete structure is short and does not allow "full recovery" of the kinetic energy of the flow to take place within the structure. The term "full recovery" refers to the kinetic energy associated with the high velocities of the jet issuing from the gate opening being converted back to potential energy in the form of depth of flow. The point of "full recovery" is the point downstream from the gate at which the flow is essentially re-established and maximum depth occurs. The principle of "full recovery" is illustrated in Figure 1 with the maximum depth of flow, and consequently "full recovery", occuring at y_d.

The measurement of water level at the scour hole is influenced by flow conditions in the structure and added dissipation of energy at the scour hole. To include the scour hole in the flow measurement system would present many problems and would require extensive calibration work because of the variability of the size of the scour holes and the effect of downstream conditions on the dissipation of energy at the scour hole. Although these problems could be overcome in the laboratory, the cost of such a study would be many times the

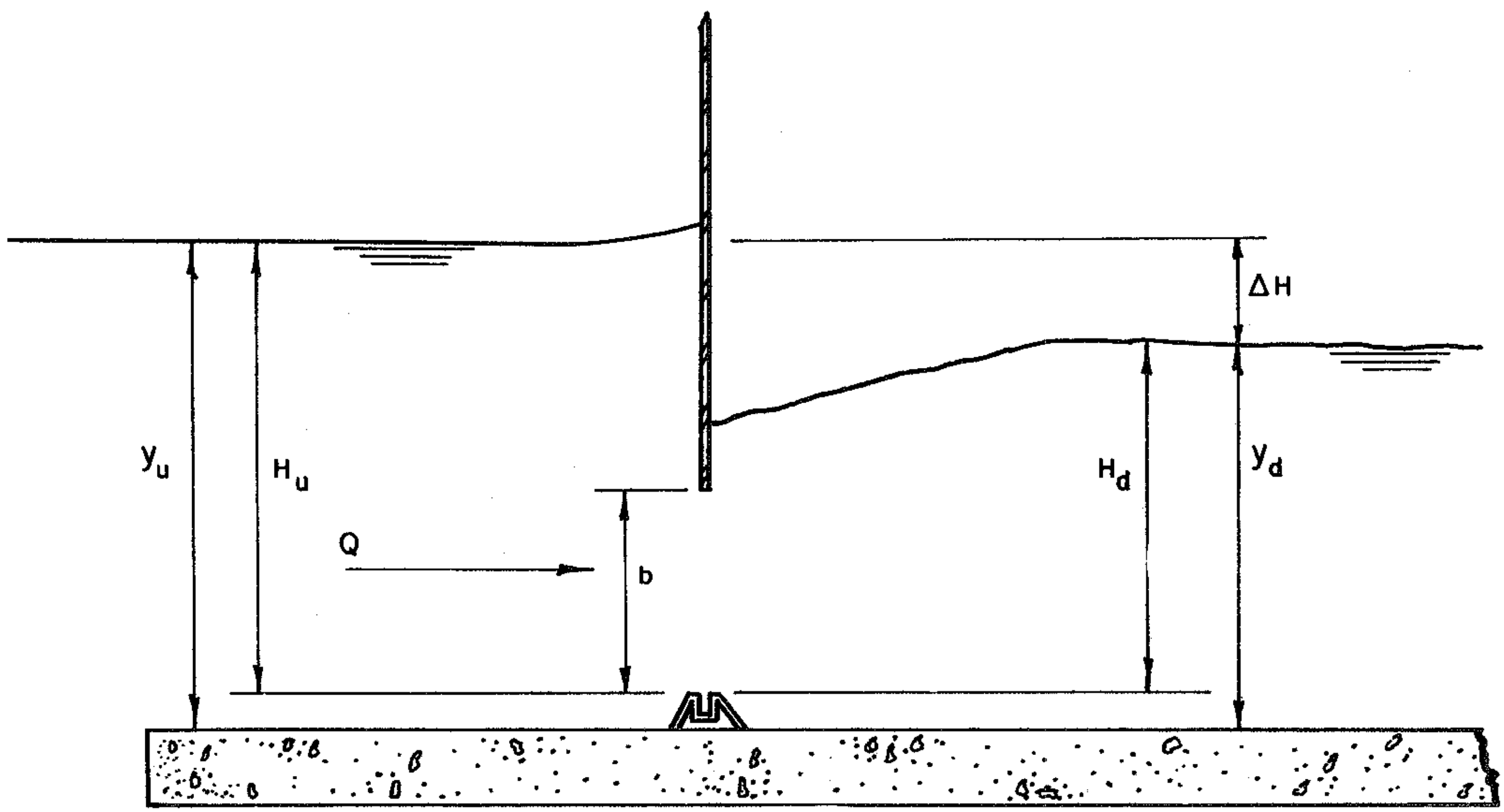

Figure 1. Definition sketch

cost of the research effort reported herein. In order to obtain a general calibration of the gate structure system, a rigid channel was placed downstream from the model gate structure. The rigid channel, in effect, was comparable to increasing the length of the concrete gate structure. This system allowed "full recovery" to occur in the channel.

The slide gate has steel angles attached around its periphery, which act as guides during the operation of the gate. These angles are located on only one face of the gate. The gates have been placed in the structure with the angles facing either upstream or downstream in a more-or-less random fashion. The water users have observed that for the same change in water surface elevation upstream and downstream from the gate, and with the same height of gate opening, the discharge will be greater with the gate angles facing upstream. Consequently, it was necessary that the calibration of the gate structure system include both conditions.

THEORY

Calibration of the gate structure used by the D. M. A. D. Company required that a model analysis be utilized in order to cover the desired flow range. After taking into account the capabilities of the laboratory equipment, it was decided to construct a model which would be geometrically similar and half the size of the field structure. Gravity flow exists both in the prototype and the model and therefore, gravity forces will be predominant in describing the flow characteristics. The characteristics of gravity flow are best described by the Froude number. Consequently, the model utilized in this study is referred to as a Froude model.

The Froude number is defined by,

$$F = \frac{V}{(gL)^{1/2}} \quad \ldots \ldots (1)$$

where,

V = average velocity of flow, feet per second

g = acceleration due to gravity, 32.2 feet per second^2

L = length, feet

The length that is normally used to evaluate the Froude number is the depth of flow.

The testing program was designed to gather data regarding the Froude number, change in water surface elevations upstream and downstream from the gate, and relative submergence. These data would then be utilized in obtaining the coefficient of discharge of the system. In order that data taken on the model can be directly applied to the prototype gate structure, it is necessary that measured quantities be combined into dimensionless terms or parameters as follows,

$$F_b = f\left(\frac{\Delta H}{b}, \frac{H_d}{b}, C_d\right) \quad \ldots \ldots (2)$$

also, from a knowledge of previous research work,

$$F_b = C_d \quad f\left(\frac{\Delta H}{b}, \frac{H_d}{b}\right)$$

where,

F_b = Froude number evaluated at the gate

ΔH = difference in upstream water surface elevation and downstream water surface elevation after full recovery

b = height of gate opening

H_d = depth of flow downstream from the gate after full recovery and using the gate sill as a datum

C_d = coefficient of discharge of system.

The Froude number evaluated at the gate is defined as the Froude number of the flow just as it passes under the gate and is arrived at as follows,

$$F = \frac{V}{(gL)^{1/2}} \quad \text{(1)}$$

The depth of flow is used as the length measurement in Equation 1. The depth, as the flow passes under the gate, is the height of gate opening. Thus, F_b can be expressed as follows,

$$F_b = \frac{V}{(gb)^{1/2}}$$

Since the flow rate, Q, is equal to the cross-sectional area of flow times the average velocity in the cross-section,

$$Q = AV \text{ or } V = Q/A$$

substituting,

$$F_b = \frac{Q}{A(gb)^{1/2}}$$

also,

$A = wb$, where w is the width of the gate. Replacing A by wb,

$$F_b = \frac{Q}{wb\,(gb)^{1/2}} \quad \ldots \ldots (3)$$

The basic measurements in the model are converted to corresponding measurements in the prototype by use of the Froude number. Throughout this report, the subscript p refers to a prototype quantity whereas, the subscript m refers to a model quantity. The subscript r refers to the ratio of the prototype quantity divided by the model quantity. Since, as mentioned above, the model was constructed one-half the size of the field structure because of laboratory limitations, the length ratio will be equal to two. Since the width of the prototype gate is 3 feet, the width of the gate utilized in the model was 1.5 feet.

$$L_r = L_p/L_m = 2$$

$$L_p = 2\,L_m \quad \ldots \ldots (4)$$

from $F = \frac{V}{(gL)^{1/2}}$

we obtain

$$F_r = \frac{V_r}{(g_r\,L_r)^{1/2}}$$

and since

$$F_r = 1 \text{ and } g_r = 1$$

$$\frac{V_r}{L_r^{\;1/2}} = 1$$

or

$$V_r = L_r^{1/2} = 2^{1/2} = 1.41$$

$$V_p = 1.41\ V_m \quad \ldots\ldots\ldots\ldots (5)$$

since

$$Q = A\ V$$

then

$$Q_r = A_r V_r = L_r^2\ L_r^{1/2}$$

$$Q_r = L_r^{5/2} = 2^{5/2} = 5.66$$

$$Q_p = 5.66\ Q_m \quad \ldots\ldots\ldots\ldots (6)$$

TESTING PROCEDURE

The model was placed in a flume five feet wide and five feet deep. In order to more nearly simulate channel conditions in the field, false sidewalls were constructed both upstream and downstream from the gate structure, thereby reducing the width of the approach and exit channels to approximately three feet. Staff gages were placed both upstream and downstream from the gate and on both sides of the flume. The flow rate was determined by use of weighing tanks.

The data were obtained by three observers acting independently of one another. For each run, the height of gate opening and the discharge rate were fixed. Also, the depth of submergence was roughly indicated for each run. The depth of submergence was established by adjusting the tailgate located at the lower end of the flume. Then, for

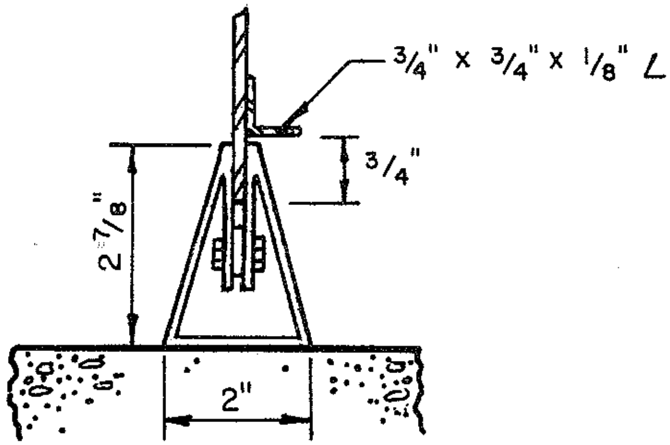

Section A-A

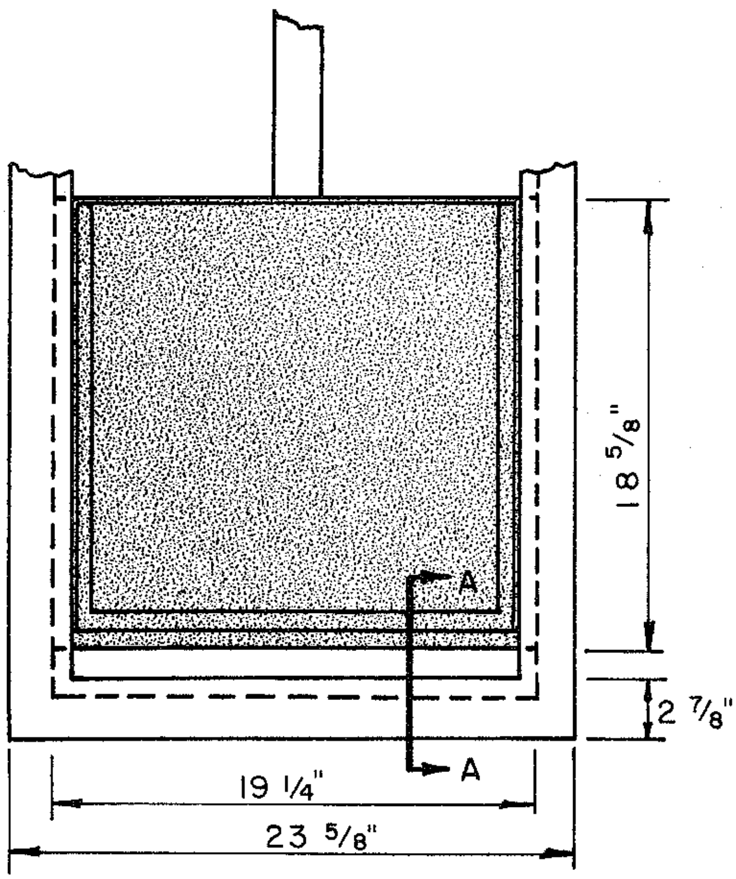

Front

Figure 2 Details of model gate

each run, each of the three observers measured the discharge rate and the staff gages. Each observer was unaware of the data taken by the others. The data were later compiled on a single data sheet, and the three measurements of each quantity were averaged. The primary advantage of this system of data gathering was that it quickly disclosed any discrepancies in the measurements.

DATA ANALYSIS

The data were initially analyzed in two different forms. First of all, F_b was plotted against $\Delta H/b$ on log-log paper. The value of H_d/b was placed alongside each of the plotted points. A plot was prepared for the gate angles facing downstream and then a separate plot was prepared for the gate angles facing upstream. The lines of best fit for values of H_d/b = 1.5, 2.0, 3.0, and 4.0 were then drawn (see Figures 3 and 4 for the results of the final plots). It was immediately apparent that the slope of these lines was 0.50, which correspond with predictions based on the results of previous researchers, and an equation was written for each value of H_d/b, which had the form

$$F_b = C_F \, (\Delta H/b)^{1/2} \quad \ldots \quad (7)$$

where C_F is the intercept of F_b for $\Delta H/b$ equal to 1.0.

$$\frac{Q}{wb\,(gb)^{1/2}} = C_F \, (\Delta H/b)^{1/2}$$

$$Q = C_F \, A \, (g \Delta H)^{1/2} \quad \ldots \quad (8)$$

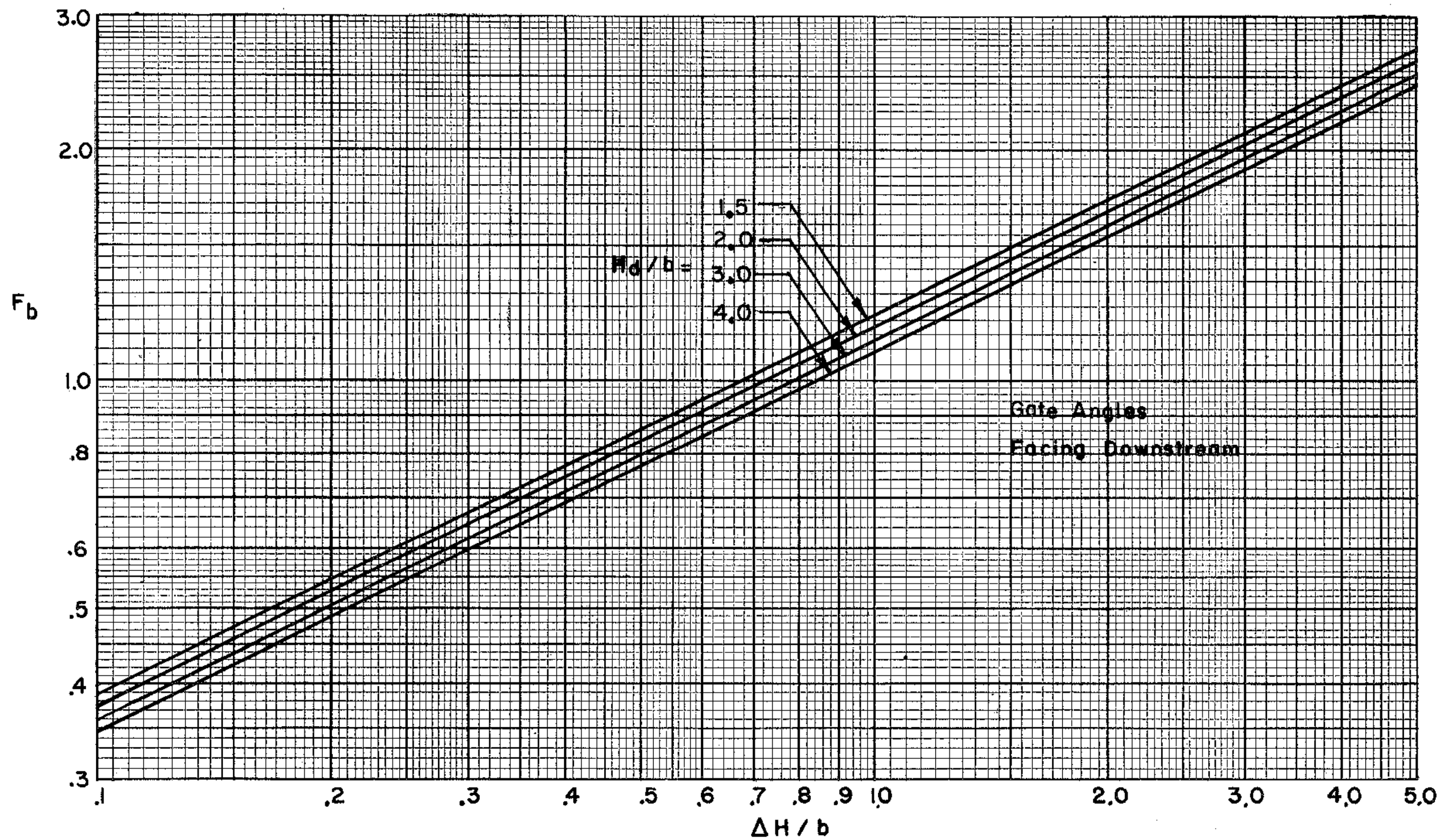

Figure 3 Plot of F_b against $\Delta H/b$
Gate angles facing downstream

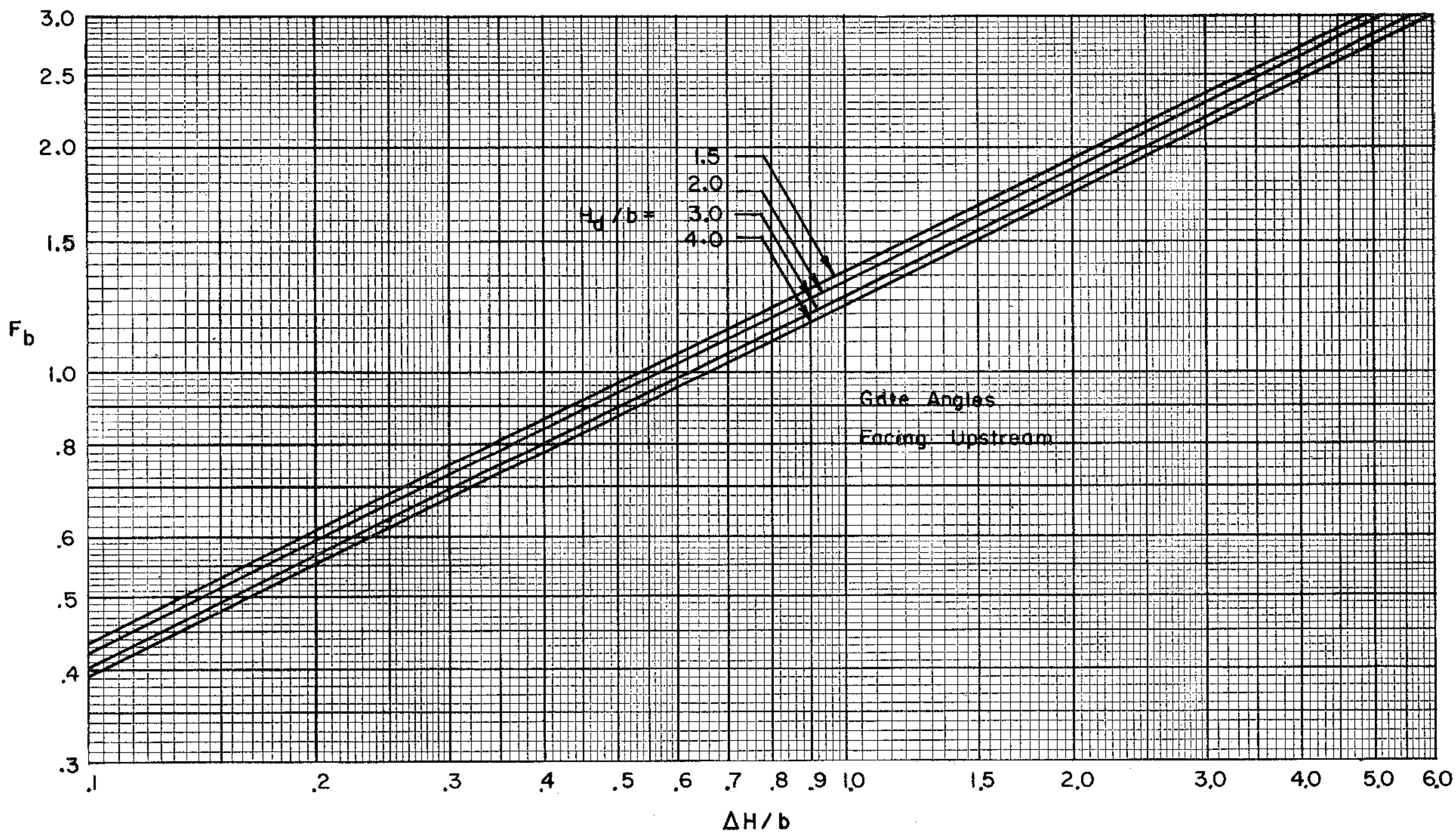

Figure 4. Plot of F_b against $\Delta H/b$
Gate angles facing upstream

Equation 8 can be compared with the equation listed in many references,

$$Q = C_d A (2 g \Delta H)^{1/2} \quad \ldots \quad (9)$$

Setting the right sides of Equations 8 and 9 equal to one another,

$$C_d A (2 g \Delta H)^{1/2} = C_F A (g \Delta H)^{1/2}$$

which reduces to

$$C_d = C_F / (2)^{1/2} = C_F / 1.41 \quad \ldots \quad (10)$$

Values of C_F, and consequently C_d, were obtained for each of the values of H_d/b equal to 1.5, 2.0, 3.0, and 4.0. A plot of C_d against H_d/b was then prepared (see Figures 7 and 8 for the final plots).

The data were next analyzed by plotting Q against ΔH on log-log paper for each height of gate opening, b. The value of H_d was written alongside each plotted point. Straight lines of best fit were drawn for various values of H_d. Again, the straight lines had a slope of 0.50 (see Figures 5 and 6 for the final plots). The variation in slope actually ranged from 0.48 to 0.52. Consequently, all of the lines were drawn with a slope of 0.50. Thus, a family of equations could be written for each value of b with each equation corresponding to a different value of H_d (and consequently, H_d/b). These equations were of the form,

$$Q = C_Q (\Delta H)^{1/2} \quad \ldots \quad (11)$$

where C_Q is the intercept of Q for ΔH equal to 1.0. Setting the right sides of the Equations 9 and 11 equal to one another,

$$C_d A (2 g \Delta H)^{1/2} = C_Q (\Delta H)^{1/2}$$

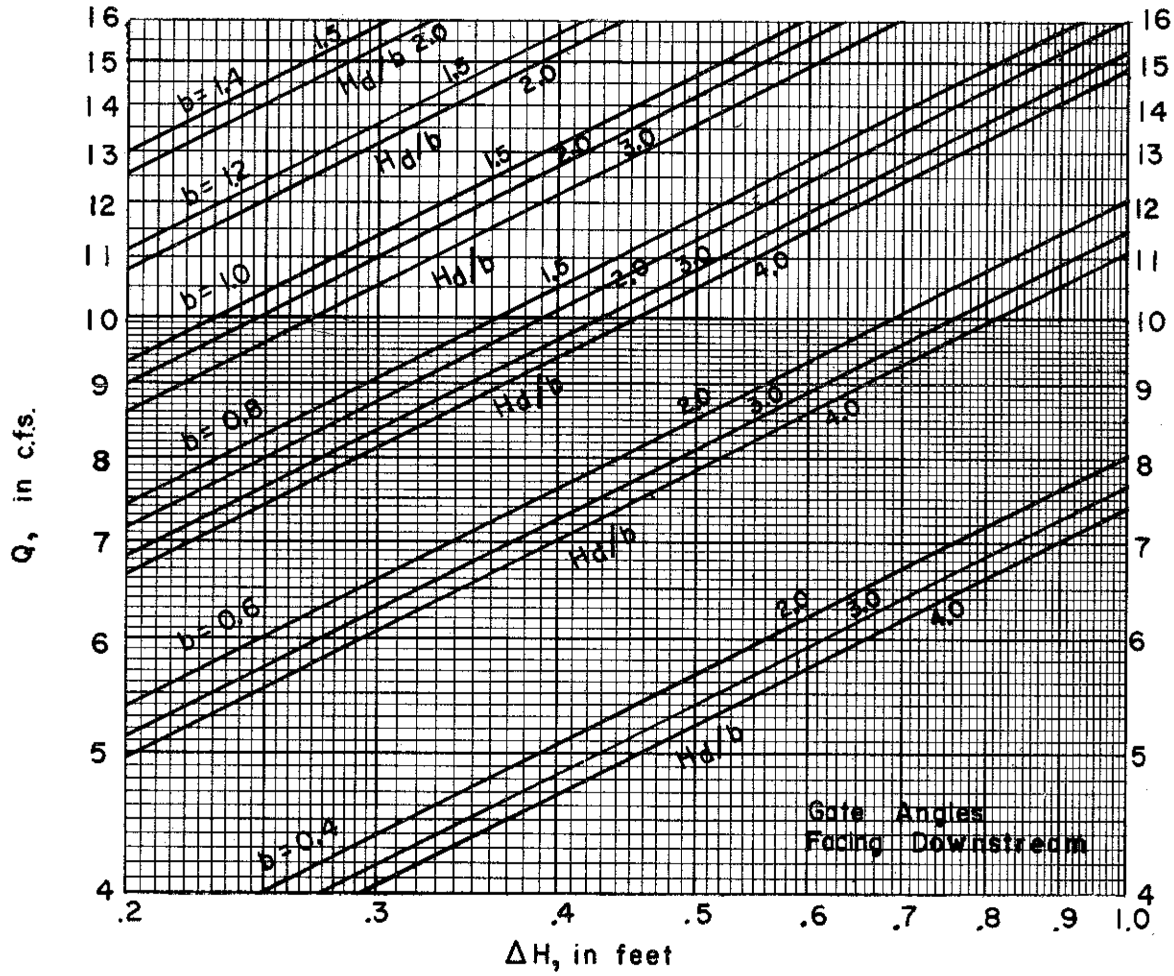

Figure 5. Plot of Q against ΔH
Gate angles facing downstream

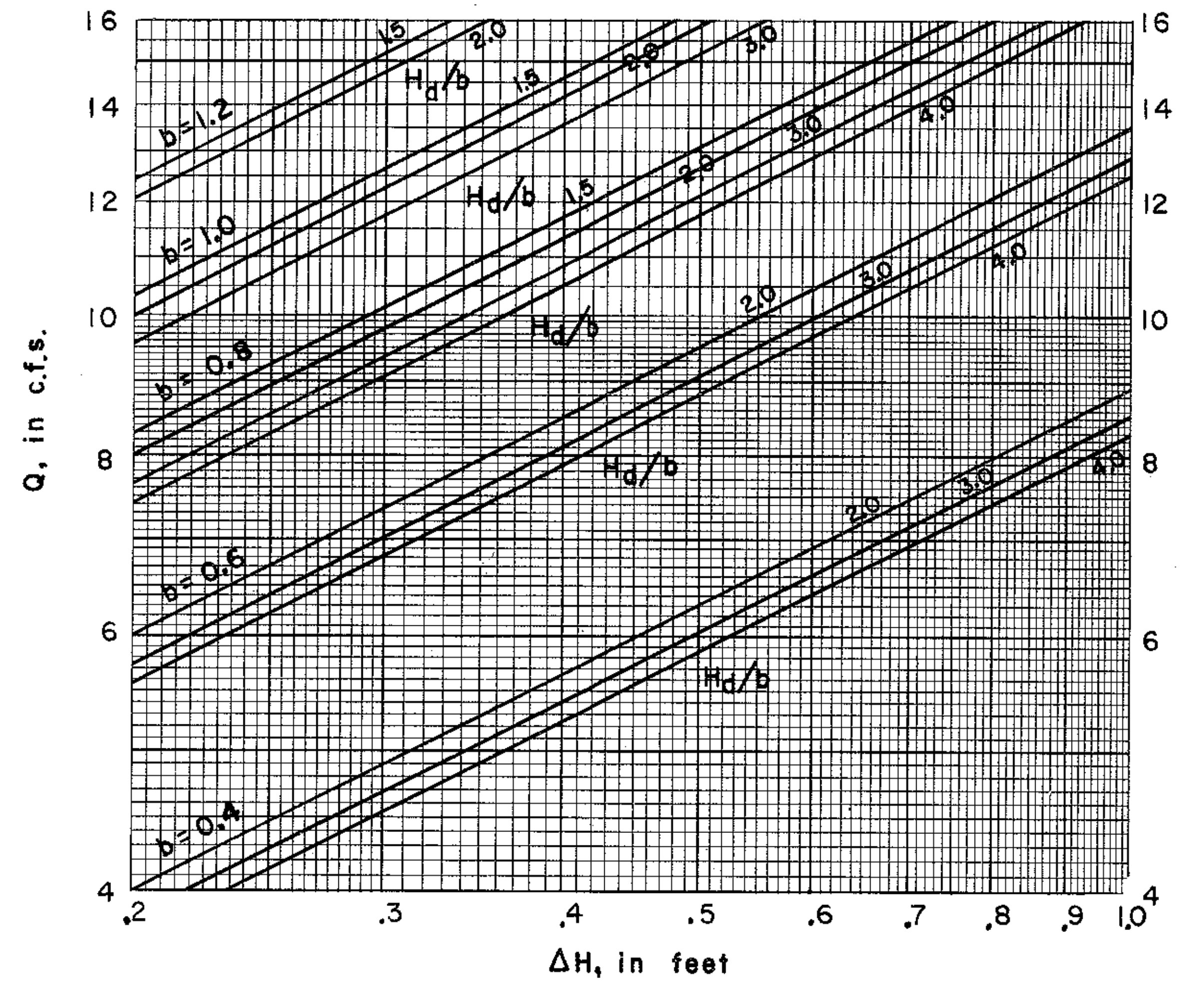

Figure 6. Plot of Q against ΔH

Gate angles facing upstream

which reduces to

$$C_d = \frac{C_Q}{A(2g)^{1/2}} = \frac{C_Q}{8.03A} \quad \ldots\ldots\ldots\ldots (12)$$

For each height of gate opening, values of C_Q corresponding to various values of H_d (or H_d/b) were obtained, from which C_d was computed. A plot of C_d versus H_d/b was then prepared for each of the values of b equal to 0.4, 0.6, 0.8, 1.0, 1.2, and 1.4 feet. For the condition of the gate angles facing upstream, data were not obtained for a height of gate opening of 1.4 feet. The results listed in the following section can be used to obtain this data.

RESULTS

The results of the plots of C_d against H_d/b by the two different methods described above were compared and a composite plot was obtained. As can be observed from Figure 7, one curve was obtained for the condition of the gate angles facing downstream and a second curve was obtained for the condition of the gate angles facing upstream.

The curves of C_d against H_d/b were next plotted on log-log paper in an attempt to express C_d as a function of H_d/b. The results of the plotting are depicted in Figure 8. For the gate angles facing downstream, C_d and H_d/b can be related by,

$$C_d = \frac{0.90}{(H_d/b)^{1/9}} \quad \ldots\ldots\ldots\ldots (13)$$

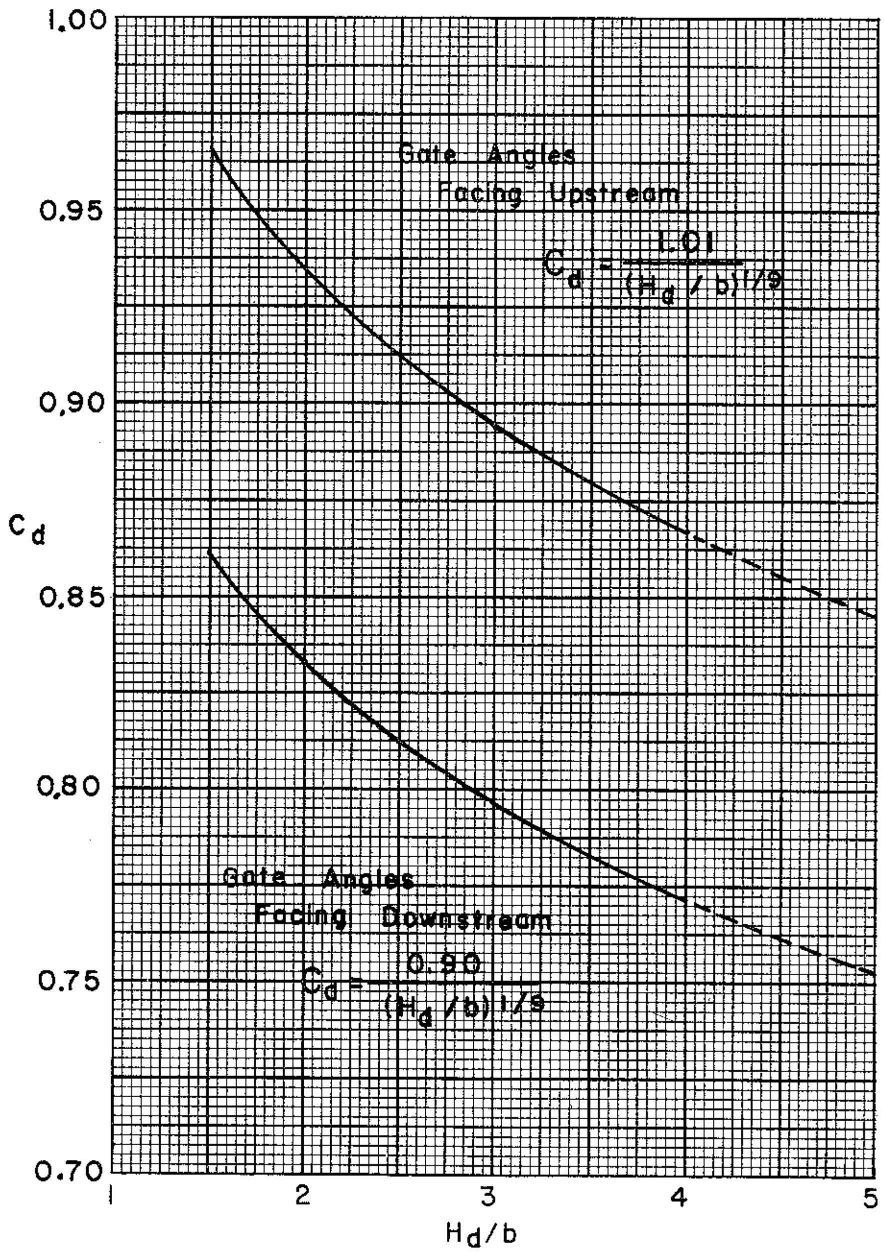

Figure 7 Effect of relative submergence on the coefficient of discharge

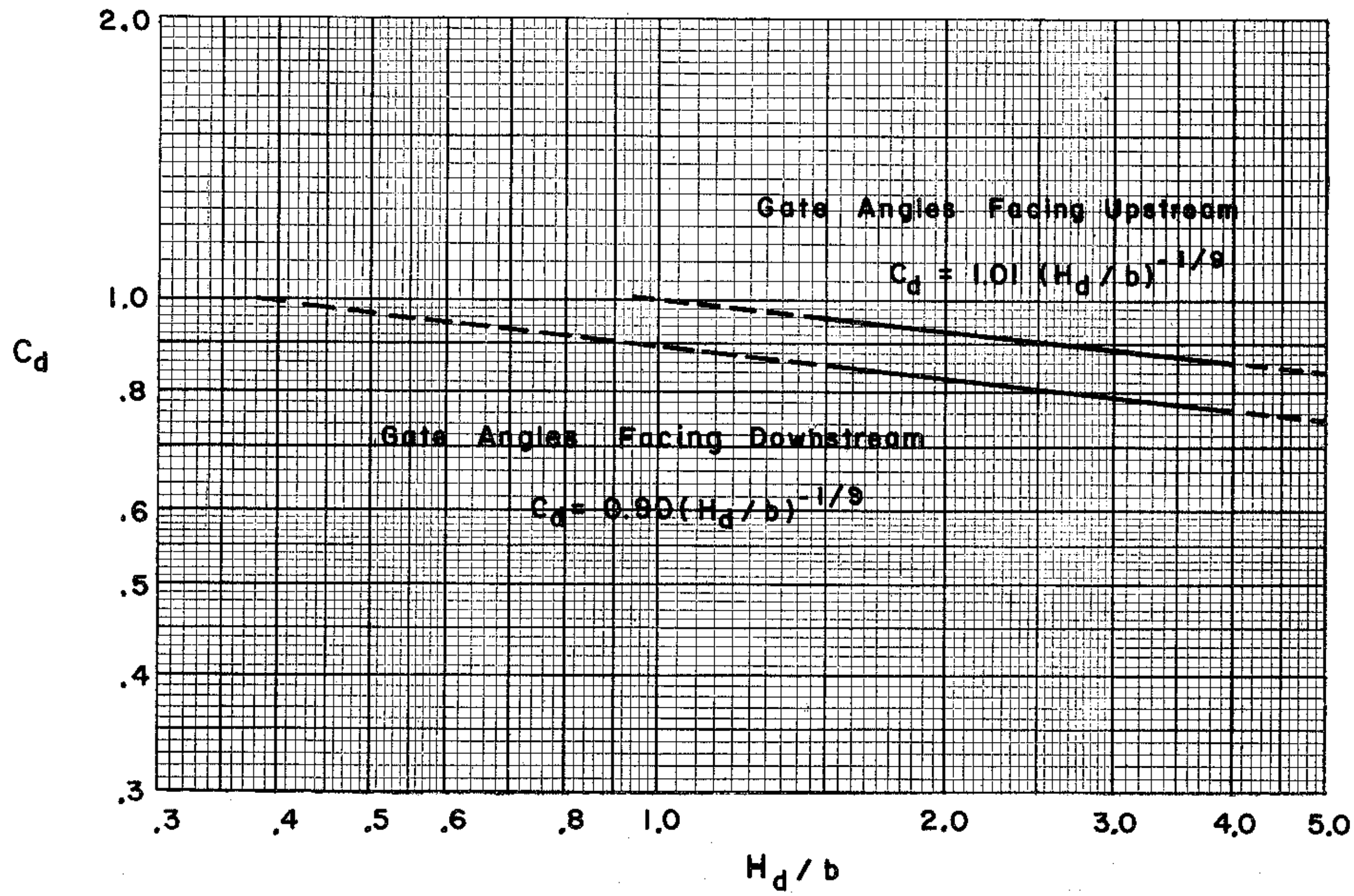

Figure 8 Plot of C_d against H_d/b

For the gate angles facing upstream, C_d and H_d/b are related by

$$C_d = \frac{1.01}{(H_d/b)^{1/9}} \qquad (14)$$

The relationships for C_d are empirical and consequently, apply only to the gates under study.

The results of the entire experimental program can be expressed by two equations. With the gate angles facing downstream,

$$Q = \frac{0.90}{(H_d/b)^{1/9}} \; wb\,(2g\Delta H)^{1/2} \qquad (15)$$

$$= \frac{7.23\, wb\,(\Delta H)^{1/2}}{(H_d/b)^{1/9}}$$

With the gate angles facing upstream,

$$Q = \frac{1.01}{(H_d/b)^{1/9}} \; wb\,(2g\Delta H)^{1/2} \qquad (16)$$

$$= \frac{8.11\, wb\,(\Delta H)^{1/2}}{(H_d/b)^{1/9}}$$

The curves shown in Figures 5 and 6 have been obtained from Equations 15 and 16.

DISCUSSION OF RESULTS

The results of this researchproject are most gratifying from three aspects.

1. The plots of log F_b against log $\Delta H/b$, and also the plots of log Q against log Δ H resulted in straight lines having a slope of 0.50 for various values of relative submergence, H_d/b.
2. A relationship between the coefficient of discharge, C_d, and the relative submergence, H_d/b, was obtained.
3. A simple equation resulted for like boundary conditions (gate angles facing downstream or gate angles facing upstream) which related the discharge, height of gate opening, difference in water surface elevations upstream and downstream from the gate, and relative submergence.

A slope of 0.50 in the plots of log F_b against log $\Delta H/b$ and log Q against log Δ H was expected since the theoretical equation (Equation 9) shows that the discharge is a function of the square root of the difference in water surface elevations upstream and downstream from the gate. Some investigators (2, 12, 13) have calibrated gate structures and have arrived at slopes varying from 0.343 to 0.49 (12, 13), and 0.504 to 0.570 (2). Other investigators (1*, 2**, 3, 7, and 9), taking into account the degree of submergence, have obtained excellent results using the square root of the difference in water surface elevations upstream

---

* Discussion by Henry in reference 1
** Discussion by Hurst in reference 2

and downstream from the gate.

Wadsworth (12) reports that originally canal headgates similar to those under study in this report, but constructed of wood, were used as measuring devices with a coefficient of discharge equal to 0.61. It was, however, soon realized that this figure was too low, and figures of 0.65 to 0.85 were used. Wadsworth then calibrated a wooden gate structure (12, 13) having a wooden gate two feet wide. His results showed a variation in C_d from 0.75 to 0.93.

The investigations of Blaisdell (2) showed a variation in C_d from 0.699 to 1.020 for the model of the Tremont gates at Lowell, Massachusetts. The model studies of the Aswan sluices in Egypt by Hurst (2) resulted in values of C_d ranging from 0.700 to 0.986 for submerged flow conditions.

The variation of the coefficient of discharge with the degree of submergence has been expressed in many forms by previous researchers (1*, 2**, 3, 7, 8, and 9). Of particular interest is the form chosen by Robin (7), who presents his data in the same form as Figure 7. Robin used this method of presentation to compare the results of his work with earlier research efforts of Addison. The curves shown by Robin have the same shape as the curves resulting from the present study and illustrated in Figure 7.

---

* Discussion by Henry in reference 1
** Discussion by Hurst in reference 2

RECOMMENDATIONS

Research has been conducted on the gate structure system used by the D. M. A. D. Company. The research effort has been aimed at calibrating the gate structure system so that it can be used for obtaining accurate flow measurements. The accuracy of the system in determining flow rates has been found to be dependent upon a number of factors. The intelligent use of the data listed in this report requires that these factors, which are listed below in the form of guidelines, be taken into account.

1. The depth of flow downstream from the gate, H_d, should be measured at the point where "full recovery" of the kinetic energy (maximum depth of flow downstream from the gate) has taken place.
2. The distance downstream from the gate at which "full recovery" takes place varies considerabley with the flow conditions. For the particular gate structure system studied, this distance can be expected to be two to eight feet downstream from the gate. The distance will be a minimum for the lower flow rates and for the higher values of relative submergence, H_d/b.
3. The depth of flow upstream from the gate, H_u, should be measured one to two feet away from the gate. The depth

of flow cannot be measured in the immediate vicinity of the gate because of the pile-up against the gate due to the conversion of velocity head to depth (see Figure 1).

4. The differences in water surface elevations upstream and downstream from the gate, ΔH, should be a minimum of 0.2 feet.

5. The heights of gate opening, b, studied under this research project covered the range 0.4 feet to 1.4 feet.

6. The minimum submergence studied for each gate opening was $H_d = b + 0.5$. The minimum depth of submergence, H_d, that should be allowed in the field when using this data to determine the discharge is the greater of (a) the height of gate opening, b, plus 0.5 feet ($H_d = b + 0.5$), or (b) one and a half times the height of gate opening, b ($H_d = 1.5b$).

7. The general equations (Equations 15 and 16) should only be used for values of relative submergence, H_d/b, ranging from 1.5 to 5.0.

8. As a general rule, the greater the value of relative submergence, H_d/b, the more accurate will be the discharge measurement.

APPENDIX

DATA SHEETS

Table Data: Gate angles facing downstream

Run No.	b_m ft	Q_m cfs	$(H_u)_m$ ft	$(H_d)_m$ ft	$(\Delta H)_m$ ft	b_p ft	Q_p cfs	$(H_u)_p$ ft	$(H_d)_p$ ft	$(\Delta H)_p$ ft	F_b	$\frac{\Delta H}{b}$	$\frac{H_d}{b}$
1	0.3	0.711	0.645	0.590	0.055	0.6	4.024	1.290	1.180	0.110	0.503	0.103	1.97
2	0.3	0.710	0.832	0.776	0.056	0.6	4.018	1.664	1.552	0.112	0.503	0.186	2.59
3	0.3	0.707	1.041	0.978	0.063	0.6	4.002	2.082	1.956	0.126	0.550	0.210	3.25
4	0.3	0.711	1.339	1.274	0.065	0.6	4.024	2.678	2.548	0.130	0.503	0.216	4.26
5	0.2	0.712	0.586	0.458	0.128	0.4	4.030	1.172	0.916	0.256	0.930	0.640	2.29
6	0.2	0.712	0.786	0.648	0.138	0.4	4.030	1.572	1.296	0.276	0.930	0.690	3.26
7	0.2	0.713	1.113	0.969	0.144	0.4	4.036	2.226	1.938	0.288	0.935	0.720	4.85
8	0.2	0.713	1.416	1.266	0.150	0.4	4.036	2.832	2.532	0.300	0.935	0.750	6.34
9	0.2	1.020	0.765	0.468	0.297	0.4	5.773	1.530	0.936	0.594	1.335	1.480	2.34
10	0.2	1.021	0.977	0.667	0.310	0.4	5.779	1.954	1.334	0.624	1.340	1.560	3.34
11	0.2	0.993	1.194	0.876	0.318	0.4	5.631	2.388	1.752	0.636	1.305	1.590	4.38
12	0.2	0.997	1.445	1.142	0.303	0.4	5.654	2.890	2.284	0.606	1.300	1.520	5.70
13	0.3	0.989	0.678	0.570	0.108	0.6	5.608	1.356	1.140	0.216	0.704	0.360	1.90
14	0.3	0.989	0.885	0.770	0.115	0.6	5.608	1.770	1.540	0.230	0.701	0.384	2.57
15	0.3	0.990	1.079	0.958	0.121	0.6	5.610	2.158	1.916	0.242	0.697	0.403	3.19
16	0.3	0.971	1.386	1.266	0.120	0.6	5.490	2.772	2.532	0.240	0.685	0.400	4.22
16'	0.3	0.999	1.404	1.274	0.130	0.6	5.654	2.808	2.548	0.260	0.710	0.433	4.25
17	0.4	1.008	0.714	0.657	0.057	0.8	5.705	1.428	1.314	0.114	0.466	0.143	1.64
18	0.4	0.992	0.925	0.860	0.065	0.8	5.614	1.850	1.720	0.130	0.461	0.162	2.15
19	0.4	0.994	1.124	1.058	0.066	0.8	5.626	2.248	2.116	0.132	0.462	0.165	2.64
20	0.4	0.991	1.433	1.362	0.071	0.8	5.609	2.866	2.724	0.142	0.459	0.178	3.40

Table Cont.

Run No.	b_m ft	Q_m cfs	$(H_u)_m$ ft	$(H_d)_m$ ft	$(\Delta H)_m$ ft	b_p ft	Q_p cfs	$(H_u)_p$ ft	$(H_d)_p$ ft	$(\Delta H)_p$ ft	F_b	$\frac{\Delta H}{b}$	$\frac{H_d}{b}$
21	0.4	1.237	0.746	0.658	0.088	0.8	7.001	1.492	1.308	0.176	0.573	0.220	1.64
22	0.4	1.230	0.975	0.877	0.098	0.8	6.962	1.950	1.754	0.196	0.570	0.245	2.19
23	0.4	1.226	1.169	1.067	0.102	0.8	6.939	2.338	2.134	0.204	0.567	0.255	2.66
24	0.4	1.218	1.381	1.276	0.105	0.8	6.894	2.762	2.552	0.210	0.567	0.262	3.19
25	0.3	1.250	0.727	0.563	0.164	0.6	7.075	1.454	1.126	0.328	0.884	0.547	1.85
26	0.3	1.253	0.950	0.779	0.171	0.6	7.092	1.900	1.558	0.342	0.885	0.571	2.60
27	0.3	1.240	1.147	0.970	0.177	0.6	7.018	2.294	1.940	0.354	0.876	0.590	3.24
28	0.3	1.248	1.462	1.277	0.185	0.6	7.064	2.924	2.554	0.370	0.885	0.617	4.25
29	0.2	1.242	0.828	0.439	0.389	0.4	7.030	1.656	0.878	0.778	1.630	1.950	2.18
30	0.2	1.250	1.083	0.673	0.410	0.4	7.075	2.166	1.346	0.820	1.640	2.050	3.36
31	0.2	1.240	1.301	0.877	0.424	0.4	7.018	2.602	1.754	0.848	1.625	2.120	4.39
32	0.2	1.247	1.481	1.049	0.432	0.4	7.058	2.962	2.098	0.864	1.635	2.160	5.24
33	0.5	1.250	0.821	0.767	0.054	1.0	7.075	1.642	1.534	0.108	0.415	0.108	1.53
34	0.5	1.255	1.028	0.972	0.057	1.0	7.103	2.056	1.944	0.114	0.418	0.114	1.94
35	0.5	1.259	1.226	1.166	0.060	1.0	7.126	2.452	2.332	0.120	0.418	0.120	2.33
36	0.5	1.254	1.408	1.347	0.061	1.0	7.098	2.816	2.694	0.122	0.416	0.122	2.69
37	0.5	1.587	0.896	0.807	0.089	1.0	8.982	1.796	1.614	0.178	0.528	0.178	1.61
38	0.5	1.573	1.068	0.968	0.100	1.0	8.903	2.136	1.936	0.200	0.525	0.200	1.94
39	0.5	1.557	1.277	1.175	0.102	1.0	8.813	2.554	2.350	0.204	0.518	0.204	2.35
40	0.5	1.557	1.459	1.351	0.108	1.0	8.813	2.918	2.702	0.216	0.518	0.216	2.70

Table Cont.

Run No.	b_m ft	Q_m cfs	$(H_u)_m$ ft	$(H_d)_m$ ft	$(\Delta H)_m$ ft	b_p ft	Q_p cfs	$(H_u)_p$ ft	$(H_d)_p$ ft	$(\Delta H)_p$ ft	F_b	$\frac{\Delta H}{b}$	$\frac{H_d}{b}$
41	0.4	1.557	0.813	0.672	0.141	0.8	8.813	1.626	1.344	0.282	0.722	0.353	1.68
42	0.4	1.540	1.028	0.877	0.151	0.8	8.716	2.056	1.754	0.302	0.714	0.378	2.19
43	0.4	1.547	1.222	1.067	0.155	0.8	8.756	2.444	2.134	0.310	0.716	0.388	2.66
44	0.4	1.530	1.407	1.247	0.160	0.8	8.660	2.814	2.494	0.320	0.710	0.400	3.12
45	0.3	1.537	0.830	0.577	0.253	0.6	8.699	1.660	1.154	0.506	1.088	0.844	1.92
46	0.3	1.527	1.034	0.770	0.264	0.6	8.643	2.068	1.548	0.528	1.080	0.880	2.58
47	0.3	1.537	1.231	0.960	0.271	0.6	8.699	2.462	1.920	0.542	1.095	0.904	3.20
48	0.3	1.528	1.444	1.166	0.278	0.6	8.648	2.888	2.332	0.556	1.088	0.927	3.88
49	0.2	1.542	1.089	0.467	0.622	0.4	8.728	2.178	0.934	1.244	2.022	3.110	2.33
50	0.2	1.538	1.194	0.559	0.635	0.4	8.705	2.388	1.118	1.270	2.022	3.175	2.80
51	0.2	1.540	1.383	0.737	0.646	0.4	8.720	2.766	1.474	1.292	2.022	3.220	3.69
52													
53	0.6	1.602	0.916	0.864	0.052	1.2	9.08	1.832	1.728	0.104	0.405	0.087	1.44
54	0.6	1.597	1.132	1.076	0.056	1.2	9.04	2.264	2.152	0.112	0.403	0.093	1.79
55	0.6	1.595	1.337	1.277	0.060	1.2	9.03	2.674	2.554	0.120	0.402	0.100	2.13
56	0.6	1.598	1.458	1.390	0.068	1.2	9.05	2.916	2.780	0.136	0.403	0.113	2.32
57	0.6	1.89	0.970	0.877	0.093	1.2	10.68	1.940	1.754	0.186	0.476	0.155	1.46
58	0.6	1.89	1.194	1.096	0.098	1.2	10.68	2.388	2.192	0.196	0.476	0.163	1.82
59	0.6	1.90	1.359	1.257	0.102	1.2	10.77	2.718	2.514	0.204	0.480	0.170	2.09
60	0.6	1.89	1.462	1.356	0.106	1.2	10.68	2.924	2.712	0.212	0.476	0.177	2.26

Table Cont.

Run No.	b_m ft	Q_m cfs	$(H_u)_m$ ft	$(H_d)_m$ ft	$(\Delta H)_m$ ft	b_p ft	Q_p cfs	$(H_u)_p$ ft	$(H_d)_p$ ft	$(\Delta H)_p$ ft	F_b	$\frac{\Delta H}{b}$	$\frac{H_d}{b}$
61	0.7	1.90	1.045	0.986	0.059	1.4	10.77	2.090	1.972	0.118	0.381	0.084	1.41
62	0.7	1.90	1.174	1.109	0.065	1.4	10.77	2.348	2.218	0.130	0.381	0.093	1.58
63	0.7	1.89	1.337	1.269	0.068	1.4	10.68	2.674	2.538	0.136	0.378	0.097	1.81
64	0.7	1.89	1.476	1.402	0.074	1.4	10.68	2.952	2.804	0.148	0.378	0.106	2.00
65	0.5	1.89	0.919	0.776	0.143	1.0	10.68	1.938	1.552	0.286	0.626	0.286	1.55
66	0.5	1.88	1.118	0.967	0.151	1.0	10.65	2.236	1.934	0.302	0.626	0.302	1.93
67	0.5	1.89	1.320	1.165	0.155	1.0	10.68	2.640	2.330	0.310	0.626	0.310	2.33
68	0.5	1.89	1.430	1.273	0.157	1.0	10.68	2.860	2.546	0.314	0.626	0.314	2.55
69	0.4	1.905	0.914	0.677	0.239	0.8	10.80	1.828	1.354	0.478	0.885	0.598	1.70
70	0.4	1.90	1.419	0.872	0.547	0.8	10.77	2.438	1.744	1.194	0.885	1.492	2.18
71	0.4	1.89	1.302	1.049	0.253	0.8	10.68	2.604	2.098	0.506	0.875	0.634	2.62
72	0.4	1.90	1.463	1.204	0.259	0.8	10.77	2.926	2.408	0.518	0.885	0.647	3.02
73	0.3	1.954	0.967	0.562	0.405	0.6	11.08	1.934	1.124	0.810	1.390	1.350	1.88
74	0.3	1.93	1.239	0.798	0.441	0.6	10.95	2.478	1.596	0.881	1.370	1.470	2.56
75	0.3	1.92	1.429	0.973	0.456	0.6	10.88	2.858	1.946	0.912	1.370	1.520	3.25
76	OVERFLOW												
77	0.3	2.19	1.146	0.604	0.542	0.6	12.40	2.292	1.208	1.084	1.550	1.810	2.01
78	0.3	2.18	1.301	0.726	0.575	0.6	12.38	2.602	1.452	1.150	1.550	1.920	2.42
79	0.3	2.19	1.455	0.871	0.584	0.6	12.40	2.910	1.742	1.168	1.550	1.948	2.91
80	OVERFLOW												

Table Cont.

Run No.	b_m ft	Q_m cfs	$(H_u)_m$ ft	$(H_d)_m$ ft	$(\Delta H)_m$ ft	b_p ft	Q_p cfs	$(H_u)_p$ ft	$(H_d)_p$ ft	$(\Delta H)_p$ ft	F_b	$\frac{\Delta H}{b}$	$\frac{H_d}{b}$
81	0.4	2.18	0.963	0.656	0.307	0.8	12.38	1.926	1.312	0.614	1.015	0.768	1.64
82	0.4	2.19	1.134	0.810	0.324	0.8	12.40	2.268	1.620	0.648	1.016	0.810	2.02
83	0.4	2.18	1.276	0.946	0.330	0.8	12.38	2.552	1.892	0.660	1.015	0.825	2.36
84	0.4	2.18	1.492	1.150	0.342	0.8	12.38	2.984	2.300	0.684	1.015	0.855	2.88
85	0.5	2.19	0.948	0.759	0.189	1.0	12.40	1.896	1.518	0.378	0.730	0.378	1.52
86	0.5	2.19	1.169	0.970	0.199	1.0	12.40	2.338	1.940	0.398	0.730	0.398	1.94
87	0.5	2.20	1.366	1.161	0.205	1.0	12.45	2.732	2.322	0.410	0.732	0.410	2.32
88	0.5	2.19	1.454	1.244	0.210	1.0	12.40	2.908	2.488	0.420	0.730	0.420	2.49
89	0.6	2.20	1.001	0.873	0.128	1.2	12.45	2.002	1.746	0.256	0.556	0.213	1.46
90	0.6	2.20	1.155	1.023	0.132	1.2	12.45	2.310	2.046	0.264	0.556	0.220	1.71
91	0.6	2.19	1.283	1.147	0.136	1.2	12.40	2.566	2.294	0.272	0.554	0.226	1.91
92	0.6	2.19	1.445	1.304	0.141	1.2	12.40	2.890	2.608	0.282	0.554	0.235	2.18
93	0.7	2.19	1.038	0.958	0.080	1.4	12.40	2.076	1.916	0.160	0.439	0.114	1.37
94	0.7	2.18	1.150	1.066	0.084	1.4	12.35	2.300	2.132	0.168	0.437	0.120	1.52
95	0.7	2.18	1.253	1.165	0.088	1.4	12.35	2.506	2.330	0.176	0.437	0.126	1.67
96	0.7	2.17	1.410	1.319	0.091	1.4	12.29	2.820	2.638	0.183	0.434	0.130	1.88
97	0.7	2.49	1.078	0.964	0.114	1.4	14.10	2.156	1.928	0.228	0.499	0.163	1.38
98	0.7	2.48	1.188	1.072	0.116	1.4	14.05	2.376	2.144	0.232	0.497	0.166	1.53
99	0.7	2.48	1.287	1.166	0.121	1.4	14.05	2.574	2.332	0.242	0.497	0.173	1.67
100	0.7	2.48	1.447	1.320	0.127	1.4	14.05	2.894	2.640	0.254	0.497	0.181	1.89

Table Cont.

Run No.	b_m ft	Q_m cfs	$(H_u)_m$ ft	$(H_d)_m$ ft	$(\Delta H)_m$ ft	b_p ft	Q_p cfs	$(H_u)_p$ ft	$(H_d)_p$ ft	$(\Delta H)_p$ ft	F_b	$\frac{\Delta H}{b}$	$\frac{H_d}{b}$
101	0.8	2.50	1.140	1.061	0.079	1.6	14.15	2.280	2.122	0.158	0.406	0.099	1.32
102	0.8	2.50	1.265	1.177	0.088	1.6	14.15	2.530	2.354	0.176	0.406	0.110	1.47
103	0.8	2.50	1.343	1.251	0.092	1.6	14.15	2.686	2.502	0.184	0.406	0.115	1.57
104	0.8	2.50	1.433	1.339	0.094	1.6	14.15	2.866	2.678	0.188	0.406	0.118	1.68
105	0.6	2.50	1.038	0.873	0.165	1.2	14.15	2.076	1.746	0.330	0.630	0.275	1.46
106	0.6	2.49	1.182	1.013	0.169	1.2	14.10	2.364	2.026	0.338	0.625	0.282	1.69
107	0.6	2.49	1.346	1.172	0.174	1.2	14.10	2.692	2.344	0.348	0.625	0.290	1.96
108	0.6	2.50	1.481	1.302	0.179	1.2	14.15	2.962	2.604	0.358	0.630	0.298	2.17
109	0.5	2.50	1.024	0.770	0.254	1.0	14.15	2.048	1.540	0.508	0.829	0.508	1.54
110	0.5	2.50	1.177	0.920	0.257	1.0	14.15	2.354	1.840	0.514	0.830	0.514	1.84
111	0.5	2.50	1.342	1.076	0.266	1.0	14.10	2.684	2.152	0.532	0.827	0.532	2.15
112	0.5	2.50	1.442	1.170	0.272	1.0	14.15	2.884	2.340	0.544	0.830	0.544	2.34
113	0.4	2.50	1.074	0.676	0.398	0.8	14.15	2.148	1.352	0.796	1.160	0.995	1.69
114	0.4	2.50	1.219	0.809	0.410	0.8	14.15	2.438	1.618	0.820	1.160	1.025	2.02
115	0.4	2.50	1.392	0.970	0.422	0.8	14.15	2.784	1.940	0.844	1.160	1.055	2.43
116	0.4	2.49	1.466	1.036	0.430	0.8	14.15	2.932	2.072	0.860	1.160	1.075	2.59

Table Data: Gate angles facing upstream

Run No.	b_m ft	Q_m cfs	$(H_u)_m$ ft	$(H_d)_m$ ft	$(\Delta H)_m$ ft	b_p ft	Q_b cfs	$(H_u)_b$ ft	$(H_d)_p$ ft	$(\Delta H)_p$ ft	F_b	$\frac{\Delta H}{b}$	$\frac{H_d}{b}$
117	0.4	0.913	0.699	0.658	0.041	0.8	5.17	1.398	1.316	0.082	0.422	0.103	1.64
118	0.4	0.910	0.871	0.836	0.040	0.8	5.15	1.752	1.672	0.080	0.422	0.100	2.09
119	0.4	0.910	1.101	1.056	0.045	0.8	5.15	2.202	2.112	0.090	0.422	0.113	2.64
120	0.4	0.908	1.396	1.348	0.048	0.8	5.14	2.792	2.696	0.096	0.421	0.120	3.37
121	0.4	1.313	0.754	0.669	0.085	0.8	7.43	1.508	1.338	0.170	0.609	0.212	1.67
122	0.4	1.313	0.964	0.875	0.089	0.8	7.43	1.928	1.750	0.178	0.609	0.223	2.19
123	0.4	1.324	1.169	1.079	0.090	0.8	7.50	2.338	2.158	0.180	0.615	0.225	2.70
124	0.4	1.313	1.350	1.261	0.089	0.8	7.43	2.700	2.522	0.178	0.609	0.223	3.16
125	0.4	1.595	0.790	0.671	0.119	0.8	9.03	1.580	1.342	0.238	0.740	0.298	1.68
126	0.4	1.595	0.987	0.861	0.126	0.8	9.03	1.974	1.722	0.252	0.740	0.315	2.15
127	0.4	1.595	1.183	1.057	0.126	0.8	9.03	2.366	2.114	0.252	0.740	0.315	2.64
128	0.4	1.585	1.384	1.253	0.131	0.8	8.97	2.768	2.506	0.262	0.735	0.328	3.14
129	0.4	1.865	0.843	0.673	0.170	0.8	10.56	1.686	1.346	0.340	0.865	0.425	1.68
130	0.4	1.865	1.029	0.853	0.176	0.8	10.56	2.058	1.706	0.352	0.865	0.440	2.13
131	0.4	1.855	1.246	1.065	0.181	0.8	10.50	2.492	2.130	0.362	0.860	0.453	2.66
132	0.4	1.855	1.422	1.237	0.185	0.8	10.50	2.844	2.474	0.370	0.866	0.463	3.09
133	0.4	2.180	0.883	0.654	0.229	0.8	12.34	1.766	1.308	0.458	1.012	0.572	1.64
134	0.4	2.175	1.056	0.815	0.241	0.8	12.31	2.112	1.630	0.482	1.010	0.003	2.04
135	0.4	2.160	1.207	0.962	0.245	0.8	12.23	2.414	1.924	0.490	1.000	0.613	2.41
136	0.4	2.160	1.417	1.165	0.252	0.8	12.23	2.834	2.330	0.504	1.000	0.629	2.92

Table Cont.

Run No.	b_m ft	Q_m cfs	$(H_u)_m$ ft	$(H_d)_m$ ft	$(\Delta H)_m$ ft	b_p ft	Q_b cfs	$(H_u)_b$ ft	$(H_d)_p$ ft	$(\Delta H)_p$ ft	F_b	$\frac{\Delta H}{b}$	$\frac{H_d}{b}$
137	0.4	2.440	0.943	0.661	0.281	0.8	13.81	1.886	1.322	0.562	1.132	0.705	1.66
138	0.4	2.440	1.093	0.800	0.293	0.8	13.81	2.186	1.606	0.586	1.132	0.734	2.00
139	0.4	2.442	1.259	0.953	0.306	0.8	13.82	2.518	1.906	0.612	1.133	0.766	2.38
140	0.4	2.440	1.474	1.155	0.319	0.8	13.81	2.948	2.310	0.638	1.132	0.797	2.89
141	0.2	0.722	0.577	0.471	0.106	0.4	4.09	1.154	0.942	0.212	0.949	0.531	2.36
142	0.2	0.720	0.973	0.864	0.109	0.4	4.07	1.946	1.728	0.218	0.945	0.545	4.32
143	0.2	0.719	1.387	1.274	0.113	0.4	4.06	2.774	2.548	0.226	0.942	0.564	6.37
144	0.2	0.992	0.664	0.456	0.208	0.4	5.62	1.328	0.912	0.416	1.305	1.040	2.28
145	0.2	0.991	0.977	0.768	0.209	0.4	5.61	1.954	1.536	0.418	1.302	1.045	3.84
146	0.2	0.999	1.355	1.145	0.210	0.4	5.65	2.710	2.290	0.420	1.310	1.050	5.72
147	0.2	1.300	0.782	0.459	0.323	0.4	7.351	1.564	0.918	0.646	1.703	1.615	2.30
148	0.2	1.300	1.098	0.762	0.336	0.4	7.351	2.196	1.524	0.672	1.703	1.675	3.81
149	0.2	1.320	1.426	1.078	0.348	0.4	7.47	2.852	2.156	0.696	1.735	1.740	5.39
150	0.2	1.570	0.955	0.494	0.461	0.4	8.90	1.910	0.988	0.922	2.065	2.305	2.47
151	0.2	1.580	1.125	0.667	0.458	0.4	8.95	2.250	1.334	0.916	2.075	2.290	3.34
152	0.2	1.555	1.369	0.906	0.463	0.4	8.80	2.738	1.812	0.926	2.040	2.315	4.53
153	0.6	1.565	0.923	0.878	0.045	1.2	8.86	1.846	1.756	0.090	0.395	0.075	1.46
154	0.6	1.540	1.163	1.116	0.047	1.2	8.72	2.326	2.232	0.094	0.389	0.078	1.86
155	0.6	1.545	1.432	1.378	0.054	1.2	8.75	2.864	2.756	0.108	0.390	0.090	2.30

Table Cont.

Run No.	b_m ft	Q_m cfs	$(H_u)_m$ ft	$(H_d)_m$ ft	$(\Delta H)_m$ ft	b_p ft	Q_b cfs	$(H_u)_b$ ft	$(H_d)_p$ ft	$(\Delta H)_p$ ft	F_b	$\frac{\Delta H}{b}$	$\frac{H_d}{b}$
156	0.6	1.935	0.967	0.888	0.079	1.2	10.95	1.934	1.776	0.158	0.489	0.132	1.48
157	0.6	1.940	1.193	1.110	0.083	1.2	10.99	2.386	2.220	0.166	0.490	0.138	1.85
158	0.6	1.935	1.444	1.363	0.081	1.2	10.95	2.888	2.726	0.162	0.489	0.135	2.27
159	0.6	2.160	0.966	0.865	0.101	1.2	12.22	1.932	1.730	0.202	0.545	0.168	1.44
160	0.6	2.160	1.231	1.124	0.107	1.2	12.22	2.462	2.248	0.214	0.545	0.178	1.88
161	0.6	2.160	1.468	1.357	0.111	1.2	12.22	2.936	2.714	0.222	0.545	0.185	2.26
162	0.6	2.380	0.978	0.852	0.126	1.2	13.48	1.956	1.704	0.252	0.602	0.210	1.42
163	0.6	2.400	1.245	1.113	0.132	1.2	13.60	2.490	2.226	0.264	0.606	0.220	1.86
164	0.6	2.380	1.478	1.345	0.133	1.2	13.48	2.956	2.690	0.266	0.602	0.222	2.24
165	0.3	1.090	0.683	0.570	0.113	0.6	6.17	1.366	1.140	0.226	0.774	0.377	1.90
166	0.3	1.080	0.983	0.861	0.122	0.6	6.11	1.966	1.722	0.244	0.768	0.407	2.88
167	0.3	1.080	1.381	1.258	0.123	0.6	6.11	2.762	2.516	0.246	0.768	0.410	4.19
168	0.3	1.527	0.768	0.563	0.205	0.6	8.64	1.536	1.126	0.410	1.082	0.684	1.88
169	0.3	1.508	1.089	0.873	0.216	0.6	8.54	2.178	1.746	0.432	1.070	0.720	2.91
170	0.3	1.495	1.394	1.173	0.221	0.6	8.46	2.788	2.346	0.442	1.066	0.737	3.91
171	0.3	1.975	0.907	0.563	0.344	0.6	11.18	1.814	1.126	0.688	1.406	1.145	1.88
172	0.3	1.970	1.254	0.884	0.370	0.6	11.15	2.508	1.768	0.740	1.397	1.235	2.94
173	0.3	1.960	1.448	1.065	0.383	0.6	11.10	2.896	2.130	0.766	1.392	1.277	3.55

Table Cont.

Run No.	b_p ft	Q_m cfs	$(H_u)_m$ ft	$(H_d)_m$ ft	$(\Delta H)_m$ ft	b_p ft	Q_b cfs	$(H_u)_b$ ft	$(H_d)_p$ ft	$(\Delta H)_p$ ft	F_b	$\frac{\Delta H}{b}$	$\frac{H_d}{b}$
174	0.5	1.955	0.892	0.774	0.118	1.0	11.07	1.784	1.548	0.236	0.639	0.236	1.55
175	0.5	1.950	1.091	0.971	0.120	1.0	11.04	2.182	1.942	0.240	0.636	0.240	1.94
176	0.5	1.950	1.414	1.285	0.129	1.0	11.04	2.828	2.570	0.258	0.646	0.258	2.57
177	0.5	1.590	0.866	0.787	0.079	1.0	9.00	1.732	1.574	0.158	0.527	0.158	1.57
178	0.5	1.595	1.161	1.076	0.085	1.0	9.02	2.322	2.152	0.170	0.529	0.170	2.15
179	0.5	1.590	1.454	1.365	0.089	1.0	9.00	2.908	2.730	0.178	0.527	0.178	2.73
180	0.5	2.380	0.945	0.758	0.187	1.0	13.48	1.890	1.516	0.374	0.791	0.374	1.52
181	0.5	2.380	1.159	0.962	0.193	1.0	13.48	2.310	1.920	0.386	0.791	0.386	1.92
182	0.5	2.380	1.465	1.260	0.205	1.0	13.46	2.930	2.520	0.410	0.791	0.410	2.52

REFERENCES

1. Albertson, M. L., Y. B. Dai, R. A. Jensen, and H. Rouse. Diffusion of submerged jets. Trans. ASCE, 115:639-697. 1950. Disc. by J. S. Holdhusen, D. Citrini, S. Corrsin, W. D. Baines, A. Streiff, H. R. Henry, and authors.

2. Blaisdell, F. W. Comparison of sluice-gate discharge in model and prototype. Trans. ASCE, 102:544-560. 1937, Disc. by R. Boucher, H. E. Hurst, G. H. Hickox, and author.

3. Elevatorski, E. A. Discharge characteristics of irrigation delivery gates. Civil Eng. Series No. 12, Eng. Experiment Station, University of Arizona, Tucson, Arizona, March, 1958.

4. Hinds, J. Rating curves for canal headgates. Reclamation Records, 13:98-99. 1922.

5. King, H. W. Handbook of Hydraulies, Fourth Edition rev. by E. F. Brater, McGraw-Hill, 1954, pp. 3-11 to 3-15.

6. Longwell, J. S., and J. Hinds. Discharge coefficients for canal headgates. Reclamation Records, 10:475-480. 1919.

7. Robin, R. C. Discharge of submerged sluice gates. Transactions Institution of Engineers, Sidney, Australia, 20:41-52. Feb. 1939, Paper No. 643.

8. Rouse, H. Engineering Hydraulics. Wiley & Sons, 1950, pp. 536-543

9. Schmidt, M. Der Vollkommene und Unvollkommene Ausfluss Unter Schützen. (Free and submerged outflow under sluice gates). Die Bautechnik, 34(8):301-303. August 1957, Berlin.

10. Stock, E. M. Measurement of irrigation water. Bull. No. 5, Eng. Experiment Station and Cooperative Extension Service, Utah State University, Logan, Utah, June 1955.

11. U. S. Bureau of Reclamation. Water Measurement Manual. First Edition, Government Printing Office, May 1953, pp. 71-80.

12. Wadsworth, H. A. Discharge through adjustable submerged orifices. Eng. News-Record, 90(7):308-309, February 15, 1923.

13. Wadsworth, H. A. Further studies of discharge through adjustable submerged orifices. Eng. News-Record, 92(20)866-867, May 15, 1924.